Extracellular matrix of secondary lymphoid organs impacts on B-cell fate and survival

Jian Song[a,1,2], Zerina Lokmic[a,1,3], Tim Lämmermann[a,4], Julia Rolf[b,5], Chuan Wu[a,6], Xueli Zhang[a,2], Rupert Hallmann[a,2], Melanie-Jane Hannocks[a,2], Nathalie Horn[a], Markus A. Ruegg[c], Arnoud Sonnenberg[d], Elisabeth Georges-Labouesse[e], Thomas H. Winkler[f], John F. Kearney[g], Susanna Cardell[b], and Lydia Sorokin[a,2,7]

[a]Institute of Physiological Chemistry and Pathobiochemistry, Muenster University, 48149 Muenster, Germany; [b]Department of Microbiology and Immunobiology, University of Gothenburg, 40530 Gothenburg, Sweden; [c]Biozentrum, CH-4056 Basel, Switzerland; [d]Netherlands Cancer Institute, 90203, Amsterdam, The Netherlands; [e]Institut de Génétique et de Biologie Moléculaire et Cellulaire, 67404 Illkirch, France; [f]Genetics Department, University of Erlangen-Nuremburg, 91054 Erlangen, Germany; and [g]Department of Microbiology, University of Alabama at Birmingham, Birmingham, AL 35294-2182

Edited by Jason G. Cyster, University of California, San Francisco, CA, and accepted by the Editorial Board June 19, 2013 (received for review October 25, 2012)

We describe a unique extracellular matrix (ECM) niche in the spleen, the marginal zone (MZ), characterized by the basement membrane glycoproteins, laminin α5 and agrin, that promotes formation of a specialized population of MZ B lymphocytes that respond rapidly to blood-borne antigens. Mice with reduced laminin α5 expression show reduced MZ B cells and increased numbers of newly formed (NF) transitional B cells that migrate from the bone marrow, without changes in other immune or stromal cell compartments. Transient integrin α6β1-mediated interaction of NF B cells with laminin α5 in the MZ supports the MZ B-cell population, their long-term survival, and antibody response. Data suggest that the unique 3D structure and biochemical composition of the ECM of lymphoid organs impacts on immune cell fate.

B-cell development | immunology

Secondary lymphoid organs are characterized by their unique patterns of immune cell compartmentalization, which is important for their function. Over recent years, the molecular basis for these distinct compartments within lymph nodes and the spleen has been intensely studied, revealing a complex interrelationship between cell–cell adhesion molecules, cytokines, and chemotactic factors. Most such adhesive and chemotactic factors are expressed by the stromal cells of the nonhematopoietic scaffold of secondary lymphoid organs, which constitute the reticular fiber network. However, little attention has been given to the acellular component of the reticular fiber network, and relatively little is known about the nature of this extracellular matrix (ECM) compartment and its function. In most tissues the ECM acts to separate cellular compartments and provides scaffolds for the adhesion and migration of cells, in the form of basement membranes or fibrillar interstitial matrices; it provides molecular cues that control differentiation and proliferation processes and determines cell survival vs. cell death (anoikis), either by direct interaction with cells or indirectly due to its large potential to bind and present cytokines and chemotactic factors (1). Whether similar functions exist in secondary lymphoid organs remains largely unvestigated.

The reticular fiber network consists of an inner core of fibrillar collagens, ensheathed by a basement membrane layer and microfibrillar proteins, and an outer layer of reticular fibroblasts (2–4). However, the molecular constituents of these layers vary in reticular fibers of different cellular compartments, and fundamental differences exist between the lymph node and spleen (4). Apart from acting as the structural backbone and potentially also a scaffold for immigrating cells (5), the reticular fiber network functions as a conduit for small-molecular-weight (<70 kDa) soluble factors (3, 6), which, in the lymph node, permit rapid delivery of antigens and/or chemokines (5) from the periphery to the surface of high endothelial venules for recruitment of T lymphocytes (2, 3). Whether other functions exist is not clear.

Our work focuses on the ECM of the spleen, in particular the marginal zone (MZ), which is central to spleen function as it contains a specialized population of B lymphocytes exhibiting a partially activated phenotype (MZ B cells) that responds rapidly to incoming pathogens by secreting large amounts of mainly IgM in a T cell–independent manner (7). In addition, MZ B cells continuously shuttle between the MZ and lymphoid follicle carrying blood-borne antigens into the follicle for presentation by follicular dendritic cells (FDCs) to follicular (FO) B cells that, in turn, present antigen to follicular T cells and thereby also contribute to the adaptive T- and B-cell immune response (8). Crucial for these functions is the localization of MZ B cells in the MZ, situated between the marginal sinus marking the border to the lymphoid follicle and the red pulp (RP), a site of high blood flow and first encounter with blood-derived pathogens and chemotactic factors. In addition to MZ B cells, immature dendritic cells (DCs), marginal zone, and metallophilic macrophages occur at this site together with specialized stromal cells, whereas recirculating FO B cells and newly formed (NF) naive B cells, which stem from the bone marrow and replenish both MZ and FO B-cell populations, occur transiently in the MZ (9).

Several factors contribute to the localization of mature MZ B cells in the MZ, most important of which are integrin α4β1-vascular cell adhesion molecule (VCAM)-1 and leukocyte function associated antigen (LFA)-1–intracellular adhesion molecule (ICAM)-1 interactions (10), and relative levels of the chemo-

Significance

We describe a unique extracellular matrix (ECM) niche in the spleen, the marginal zone (MZ), that supports a specialized population of MZ B lymphocytes that respond rapidly to blood-borne antigens and are therefore crucial for the first line of immune defense. We show, for the first time, that both the novel 3D structure and the biochemical composition of the ECM impacts on B-cell fate and survival. Similar pericellular ECM networks occur in thymus, bone marrow, and lymph node; hence, our data are likely to have broader ramifications to the fate and survival of other immune cells.

Author contributions: R.H., T.H.W., J.F.K., S.C., and L.S. designed research; J.S., Z.L., T.L., X.Z., and M.-J.H. performed research; J.R., C.W., X.Z., R.H., N.H., M.A.R., A.S., and E.G.-L. contributed new reagents/analytic tools; J.S., Z.L., T.L., J.R., M.-J.H., T.H.W., J.F.K., S.C., and L.S. analyzed data; and J.S., Z.L., T.H.W., J.F.K., S.C., and L.S. wrote the paper.

The authors declare no conflict of interest.

This article is a PNAS Direct Submission. J.G.C. is a guest editor invited by the Editorial Board.

[1]J.S. and Z.L. contributed equally to this work.

[2]Cells-in-Motion Cluster of Excellence.

[3]Present address: Murdoch Childrens Research Institute, Melbourne, VIC 3052, Australia.

[4]Present address: Laboratory of Systems Biology, National Institute of Allergy and Infectious Diseases, National Institutes of Health, Bethesda, MD 20892-0421.

[5]Present address: Division of Cell Signalling and Immunology, Dundee University, Dundee DD1 5EH, United Kingdom.

[6]Present address: Center for Neurologic Disease Brigham and Women's Hospital, Harvard Medical School, Boston, MA 02115.

[7]To whom correspondence should be addressed. E-mail: sorokin@uni-muenster.de.

This article contains supporting information online at www.pnas.org/lookup/suppl/doi:10.1073/pnas.1218131110/-/DCSupplemental.

kines, sphingosine-1-phosphate (S1P) and CXCL13, in the circulation and in the follicle (11). However, there is comparatively little knowledge about how and indeed whether the MZ microenvironment influences MZ B-cell development or how the size of the MZ B-cell pool is regulated. During development, B-cell precursors develop in the bone marrow and move to the spleen where they constitute the newly formed immature (transitional) B cells that give rise to the mature MZ and FO B-cell populations (12). This process occurs continuously and also replenishes the MZ and FO B-cell populations in the adult. Signaling through the B-cell receptor (BCR), Notch2, the receptor for B cell–activating factor (BAFF) signaling, and the canonical NF-κB pathway has been shown to be crucial in determining MZ B-cell fate (13). In addition, factors involved in the migration and anatomical retention of MZ B cells, such as the B-cell coreceptor, CD19, that associates with the integrin-linked CD9 and CD81 tetraspanins (14, 15), or the tyrosine kinase, Pyk-2 (16), are required for establishment of the MZ B-cell population as, in their absence, no MZ B cells form but FO B cells are not affected.

We show here that the ECM also distinguishes different immune cell compartments in the spleen and promotes the B-cell population of the MZ. The MZ is revealed to be a unique ECM structure that surrounds individual stromal cells and is characterized by the presence of the basement membrane–specific molecule, laminin α5, and the heparan sulfate proteoglycan, agrin. In vivo distribution of laminin α5 and agrin precisely correlate with MZ B-cell localization. However, only reduction of laminin α5 and not agrin in the MZ of a laminin α5 conditional KO mouse results in reduced MZ B-cell numbers and concurrent increase in NF B cells migrating into the spleen from the bone marrow. In vivo and in vitro data suggest that the presence of laminin α5 in the MZ maintains the MZ B-cell compartment in an integrin α6β1–dependent manner. We show that laminin α5 also binds BAFF and leads to clustering and colocalization of integrin α6β1 and BAFF receptors on the NF B cells, thereby syngerizing with BAFF to support survival of NF B cells and the mature MZ B-cell population. Although the ECM of secondary lymphoid organs can well be envisaged as an important structural component separating different cell compartments and acting as a scaffold guiding cell movement (17), this is clear evidence that it can also directly contribute to immune cell fate and survival.

Results

Laminin α5 Is Predominantly Expressed in the MZ. Using the antibodies listed in Table 1, we characterized the ECM of the spleen, with a focus on the MZ, revealing the expression of laminin α5 (Fig. 1 *A–D*) and the heparan sulfate proteoglycan, agrin (Fig. 1 *E–G*), in the MZ. In addition, laminin α5 is strongly expressed in basement membranes of the sinus lining endothelium and of blood vessels in the RP (Fig. 1 *A–D*). By contrast, other basement membrane molecules, including nidogen 1, collagen type IV, ERTR7, and perlecan, are equally distributed throughout the MZ and the RP (Fig. S1*A*). Confocal microscopy of immunofluorescently stained sections revealed that laminin α5 and agrin colocalize in a perifollicular fibrillar network (Fig. 1 *E* and *G*), precisely coincident with IgM^{high}/IgD^{low} MZ B cells (Fig. 1 *D* and *F*) and overlapping with VCAM-1–expressing areas (Fig. 1 *H* and *I*), characteristic of the MZ. This filigree laminin α5 staining in the MZ colocalized with laminin γ1 and β1 or laminin γ1 and β2 chains, indicating the existence of laminin isoforms 511 and 521, respectively, and was distinct biochemically, and in fiber density and dimensions from the staining of reticular fibers in the follicle and in the RP (Fig. 1 *H* and *I*; Fig. S1 *A–D*). In contrast to reticular fibers of the MZ and RP, those of the white pulp (WP) contain collagens I and II, whereas ERTR 7 is present in the RP and MZ but not the B-cell zone of the follicle (4). As a consequence of these biochemical differences, fiber sizes differ in the MZ, RP, and WP, with mean diameters of <0.5 μm in the RP, 0.5–1 μm in the MZ and 1–2 μm in the WP (Fig. S1 *B–D*) (4).

Mice with enlarged MZs and higher frequencies of MZ B cells, including nonobese diabetic (NOD) and the transgenic 24αβNOD mice expressing the CD1d-restricted Vα3.2Vβ9 T-cell receptor (TCR) (18) (Fig. 2 *A* and *B*), showed a broader distribution of the laminin α5 and agrin than control C57BL/6 mice (Fig. 2*C*) that correlated with the localization of $B220^+$ cells in the MZ (Fig. 2*B*). Conversely, $CD19^{-/-}$ mice, lacking MZ B cells (19), also lacked laminin α5 in the MZ but showed no change in agrin staining (Fig. S2). ICAM-1 and VCAM-1 staining patterns did not differ from those observed in control C57BL/6 mice (Fig. S2). The closer correlation between MZ B-cell localization and laminin α5 than with agrin was confirmed in $agrin^{-/-}$ mice (20), which showed no loss of laminin α5 or disturbances in MZ B-cell localization or numbers (Fig. S2).

Reduced MZ B-Cell and Increased Newly Formed B-Cell Numbers in *Lama5*$^{-/-}$ Spleens. As mice lacking laminin α5 (*Lama5*$^{-/-}$) die embryonically (21), we generated tissue-specific *Lama5*$^{-/-}$ mice, some of which show altered laminin α5 localization in the MZ. We report here on one strain generated by crossing the Tie-2-cre transgenic strain (22) with mice carrying loxP sites flanking exon 1 of *Lama5* (Fig. S3 *A–C*). The rational for examining the spleen of the endothelial cell specific *Lama5*$^{-/-}$ mouse was based on the expression of several endothelial cell markers in stroma of the spleen (Fig. S4*A*) (4). This conditional *Lama5*$^{-/-}$ mouse showed significantly reduced laminin α5 in the MZ and in blood vessel basement membranes in the RP (Fig. 2*D*) but no difference in

Table 1. ECM primary antibodies used in immunofluorescence

Name of molecule	Antibody name/clone	Reference/source
Laminin α1	317	(32)
Laminin α2	401	(32)
Laminin α4	377	(32)
Laminin α5	504	(32)
Laminin γ1	3E10	(45)
Laminin β1	3A4	(45)
Laminin β2	Rabbit serum (domain IV)	(46)
Pan-laminin	455	(32)
Laminin 332 (composed of laminin α3,γ2,β3)	AP1002.3	ImmunDiagnostik
Nidogen 1	Rabbit serum	(47)
Nidogen 2	Rabbit serum	(48)
Agrin	204	(41)
Perlecan	A716 C11L1	(32)
Collagen type IV	AB765	(32)
Collagen type I	AB756P	Chemicon
Collagen type III	1330–01	Southern Biotech
Tenascin-C	MTN1	(49)
Fibronectin	Chicken serum (RGD-binding)	(45)

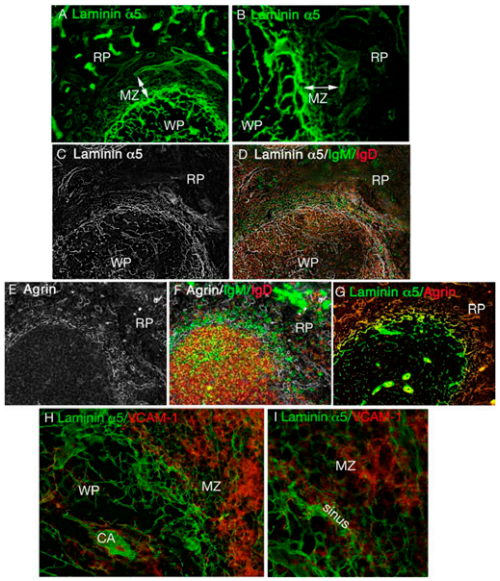

Fig. 1. Immunofluorescence staining for laminin α5, agrin, IgM^{high}/IgD^{low} MZ B cells, and VCAM-1$^+$ stromal cells in the MZ. (*A*) Anti–laminin α5 stains basement membranes of the sinus lining endothelium, blood vessels in the RP, and the reticular fibers in the WP; (*B*) higher magnification shows a filigree laminin α5 pattern in the MZ (double arrows) that is distinct from the thicker reticular fiber staining in the WP. Confocal image of a thick section (60 μm) stained for laminin α5 (*C* and *D*) or agrin (*E* and *F*) together with IgM and IgD showing colocalization of laminin α5 and agrin with IgM^{high} MZ B cells in the MZ. (*G*) Double staining for laminin α5 and agrin shows that both occur in the MZ but that laminin α5 has a more extensive distribution in the WP and in the sinus lining basement membrane. Confocal image of a thick section (60 μm) stained for laminin α5 and VCAM-1 (*H* and *I*) shows overlap of VCAM-1$^+$ stromal cells in the MZ and the laminin α5 network. CA, central artery; WP, white pulp; sinus, marginal sinus; MZ, marginal zone; RP, red pulp. Magnification: *A* and *C–G*, 100×; *B* and *H*, 200×; *I*, 400×.

agrin, VCAM-1, ICAM-1, and mucosal addressin cell adhesion molecule (MAdCAM)-1 staining compared with littermate *Lama5* floxed/floxed mice (defined as WT controls; Fig. S5*A*). The expression of other ECM molecules normally found in MZ and RP was also unaltered, as was the localization and total numbers of metallophilic macrophages antibody (MOMA)-1$^+$ sinus lining macrophages and ERTR9$^+$ MZ macrophages (Fig. S5 *A* and *B*). The residual laminin α5 staining at the marginal sinus of the *Lama5*$^{-/-}$ mouse is derived from perivascular cells (Fig. S4 *B* and *C*).

Flow cytometry revealed reduced numbers of CD23^{low}/CD21^{high} MZ B cells in the conditional *Lama5*$^{-/-}$ mice compared with WT controls and a concomitant increase in the CD21^{low}/CD23^{low} NF B cells but no differences in CD23^{high}/CD21^{low} FO B-cell numbers (Fig. 2*E*). Analyses of the blood of *Lama5*$^{-/-}$ mice confirmed the absence of circulating MZ B cells and no differences from WT littermates in circulating levels of total CD45$^+$ cells or B cells (Fig. S5*C*). However, *Lama5*$^{-/-}$ mice showed significantly reduced circulating antibody levels after immunization with NP-Ficoll, indicating an impaired immunological response to T cell–independent antigens (Fig. 2*F*).

Flow cytometry of the bone marrow for pre- and pro-B cells, newly formed immature B cells, and recirculating B cells, as determined by their B220/CD19/CD21/CD23/AA4.1/IgM profiles (12), revealed no difference between *Lama5*$^{-/-}$ and WT mice (Fig. S6*A*). Spleens of WT and *Lama5*$^{-/-}$ mice also showed similar proportions of CD19$^+$/AA4.1$^+$ immature B cells; however, *Lama5*$^{-/-}$ mice had increased proportions and absolute numbers of the "transitional" T1 population and an associated reduction in the T2 population but no change in the T3 population (Fig. S6*B*). As the T1 population represents early immigrants from the bone marrow that develop to the T2 population in the spleen, and T2 contains considerable numbers of precursors that give rise to the MZ B cells (12), this suggests a defect in T1 to T2 transition leading to a subsequent decrease in mature MZ B cells.

Functional Significance of Laminin α5 in the MZ. ***Newly formed B cells and MZ B cells show integrin-mediated binding to laminin α5.*** Flow cytometry revealed that NF, MZ, and FO B cells all express integrin subunits that constitute receptors known to recognize laminin α5, including integrins β3, αv, α5, and α6 (Fig. 3*A*; Fig. S7*A*) (23, 24). In addition, integrins α4, β1, αL, β2, and β7 were detected on NF (Fig. 3*A*) and, as previously reported (10), on MZ and FO B cells (Fig. S7*A*). Other ECM-binding receptors, including integrins α1, α2, and α7, dystroglycan, lutheran blood group glycoprotein (25), and sulphatide (3′-sulphogalactosylceramide) (26), were not detectable on the surface of NF, MZ, or FO B cells.

To test functional activity of the integrins, in vitro adhesion assays were performed. NF B cells showed high levels of binding to laminin 511/521, which exceeded the binding to VCAM-1 and was abolished by function blocking antibodies to integrins α6 and β1, suggesting involvement of α6β1 (Fig. 3*B*). MZ and FO B cells also bound laminin 511/521 but to similar levels as to VCAM-1 (Fig. 3*B*), and binding was inhibited by blocking antibodies to integrins β1 and β3 and RGD (Arg-Gly-Asp) peptide (Fig. S7*B*), suggesting involvement of integrins α5β1, αvβ3, and/or αvβ1 (23). This result was substantiated by the use of the RGD-containing laminin α5 recombinant domain IVa, which supported binding of MZ and FO B cells, but not of NF B cells, in an integrin β3– and RGD-dependent manner (Fig. 3*B*; Fig. S7*B*).

NF, MZ, and FO B cells all showed less extensive binding to agrin and no binding to fibronectin despite expression of several fibronectin receptors (including α4β1, α5β1, and αvβ3/αvβ1) and its reported expression in the spleen (27). Taken together, this suggests that mature and NF B cells can interact directly with laminin α5 but that different domains are recognized by distinct receptors on MZ and FO vs. NF B cells, resulting in transduction of different signals. In vivo dislodgement experiments performed with antibodies to integrins β1, β3, and α6, laminin α5, or combinations thereof, as previously described for anti-αL and α4 integrin antibodies (10), revealed no dislodgement of MZ or FO B cells from the spleen into the blood (Table S1), suggesting that binding to laminin α5 does not contribute to long-term localization of mature B-cell populations to the spleen.

Integrin α6β1-mediated homing of NF B cells to the laminin α5-rich MZ. The precise localization of immigrating NF B cells in the spleen is not clear due to the need to simultaneously stain for several marker molecules for their identification. We therefore used IgM$^+$CD21^{low} and AA4.1$^+$IgM$^+$ to investigate whether immature B cells and laminin α5 show any colocalization in vivo. This examination revealed the presence of IgM$^+$CD21^{low} and AA4.1$^+$IgM$^+$ cells in the MZ but also in the follicle, RP, and periarteriolar lymphoid sheaths (PALSs; Fig. 3 *C* and *D*), as reported also by others (28, 29), suggesting at least transient localization of the NF B cells in the MZ. To more precisely investigate whether NF B cells can reside in the MZ, NF cells isolated from spleens of 10-d-old mice were labeled with 5′/6′-carboxytetramethylrhodamine (TAMRA), and 5×10^6 cells per mouse were injected i.v. into mature (8–9 wk) mice; spleens were analyzed 16 h after transfer. TAMRA$^+$ NF B cells were found in the laminin α5$^+$ MZ but also the FO (at a ratio of 2:3; Fig. 3*E*); however, when NF B cells were preincubated with GoH3 (anti-integrin α6), significantly fewer TAMRA$^+$ cells localized to the MZ and more accumulated in the FO (ratio of 1:5; Fig. 3*E*). I.v.-injected TAMRA-labeled FO B cells homed almost exclusively to the follicle, and GoH3 had no effect on their localization (Fig. 3*E*). GoH3 did not affect the total number of host or donor NF or FO B cells accumulating in the spleen after transfer, indicating that only NF B-cell localization within the spleen was altered and that there was no displacement of NF or FO B cells to the circulation (Fig. S8*A*). Injection of TAMRA$^+$ NF B cells into *Lama5*$^{-/-}$ also resulted in accumulation of TAMRA$^+$ cells in the FO (Fig. S8*B*). Because *Lama5*$^{-/-}$ have some MZ B cells, this suggests that NF B cells can develop to MZ B cells outside of the MZ but that it is less efficient than in the MZ.

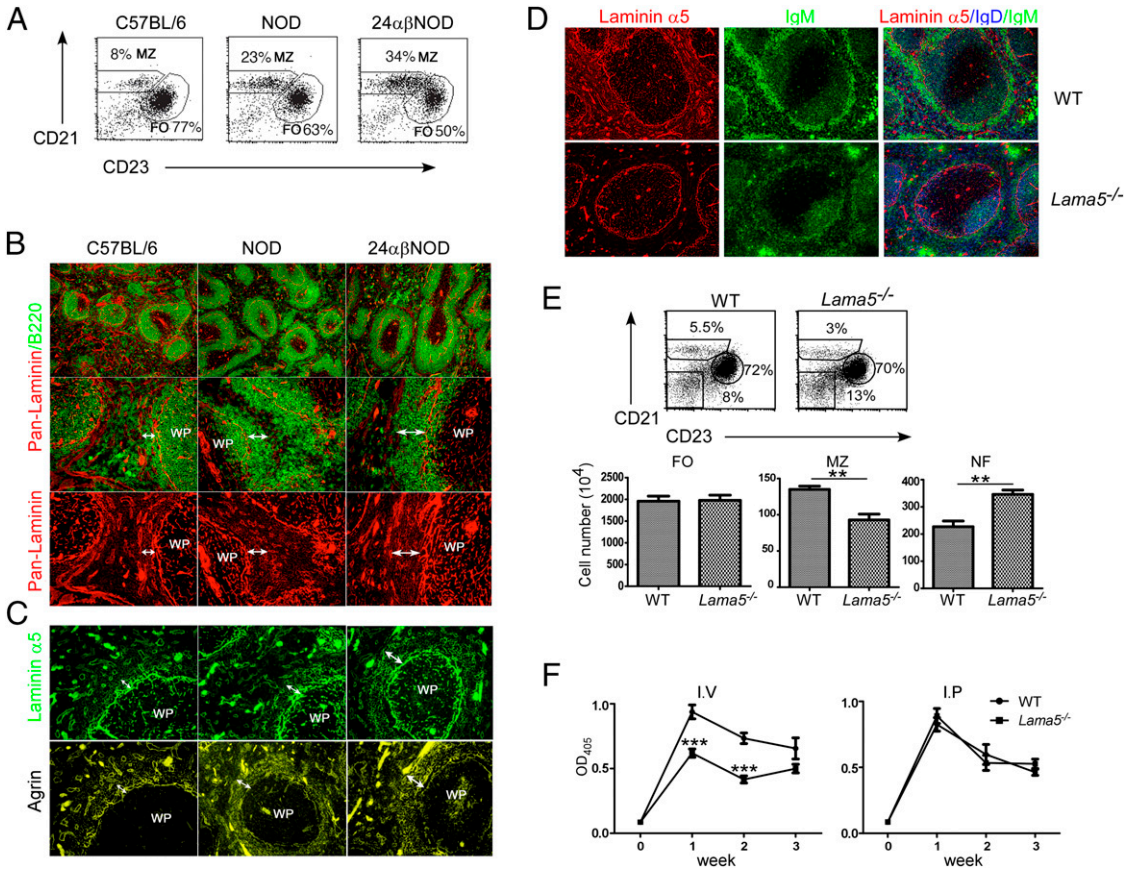

Fig. 2. Laminin α5 distribution in the MZ correlates with MZ B-cell localization and numbers. (*A*) Flow cytometry of adult spleens from C57BL/6 mice, NOD, and 24αβNOD transgenic mice showing an increase in the CD21^{high}CD23^{low} MZ B-cell population in the latter two mouse strains, and (*B*) associated expansion of immunofluorescence staining for pan-laminin and B220 in the MZ (double arrows). (*C*) Expansion of the MZ is associated with broader immunofluorescent staining for laminin α5 and agrin in the MZ of NOD and 24αβNOD mice. Magnification: top panel in *B*, 100×; otherwise, 200×. (*D*) Immunofluorescence staining of adult spleen sections from conditional *Lama5*$^{-/-}$ mice and WT littermates for laminin α5, IgM, and IgD showing reduced laminin α5 localization in the MZ and associated reduction in the IgM^{high}/IgD^{low} MZ B-cell population. Magnification, 150×. (*E*) Flow cytometry reveals lower frequencies and total numbers of MZ B cells in *Lama5*$^{-/-}$ spleens and an increase in CD21^{low}/CD23^{low} NF B cells, but no change in CD21^{low}/CD23^{high} FO B cells. Gated on CD19^{+} cells. Quantitative data shown is for three experiments with four to five mice per experiment. (*F*) Circulating IgM levels in *Lama5*$^{-/-}$ mice and WT littermates in response to i.v. or i.p. immunization with T cell–independent antigen (NP-Ficoll). Data shown are means ± SEM from six *Lama5*$^{-/-}$ mice and WT littermates and three independent experiments. $^{**}P < 0.01$; $^{***}P < 0.001$.

Integrin α6$^{-/-}$ Bone Marrow Chimera Mice Phenocopy the *Lama5*$^{-/-}$ Phenotype. In view of the high expression of integrin α6β1 on NF B cells and its ability to mediate binding to laminin α5, we generated bone marrow chimeric mice carrying integrin α6$^{-/-}$ (*Itga6*$^{-/-}$) bone marrow and followed the in vivo reconstitution of splenic B-cell populations, which was necessary as *Itga6*$^{-/-}$ mice die at birth (30). As in the conditional *Lama5*$^{-/-}$ mouse, the *Itga6*$^{-/-}$ chimeras showed reduced MZ B-cell numbers and increased NF B cells, but no difference in FO B-cell numbers (Fig. 4*A*). The antibody response of the *Itga6*$^{-/-}$ chimeras to NP-Ficoll was also impaired, as for the *Lama5*$^{-/-}$ mouse (Fig. 4*B*).

Analysis of the AA4.1 population, as a marker of immature B cells, revealed an enhanced proportion and absolute numbers of the CD19^{+}CD23^{-} T1 population and a reduced CD19^{+}CD23^{+} T2/T3 population in the spleen, but no defect in immature B cells in the bone marrow (Fig. S9 *A* and *B*), suggesting a similar block in the formation of MZ precursor cells only in the spleen as occurs in mice lacking laminin α5 in the MZ.

Competitive bone marrow reconstitution studies performed with a 1:1 ratio of CD45.1^{+} WT:CD45.2^{+} *Itga6*$^{-/-}$ bone marrow cells did not show any developmental defect in bone marrow B-cell or myeloid populations in the absence of integrin α6 (Fig. S10 *A* and *B*). However, in the spleen, *Itga6*$^{-/-}$ precursors accumulated at the NF B-cell stage and were less efficient than WT precursors in establishment of the MZ B-cell population, but could constitute the FO B-cell population as efficiently as WT cells (Fig. 4*C*).

Laminin α5 Promotes MZ B-Cell Survival. To investigate whether integrin α6β1-mediated interaction with laminin α5 influences long-term survival of the mature MZ B cells, flow cytometry for proportions of TUNEL-positive cells was performed as a measure of apoptosis, revealing enhanced apoptosis of MZ B cells in both conditional *Lama5*$^{-/-}$ and *Itga6*$^{-/-}$ chimeric spleens (Fig. 5*A*). This result was confirmed by quantitative RT-PCR (qRT-PCR) performed on sorted MZ, FO, and NF B cells, revealing down-regulation of the antiapoptotic (Bcl-XL, Bcl-2) and up-regulation of proapoptotic (Bim) genes in MZ B cells in both conditional *Lama5*$^{-/-}$ (Fig. S11*A*) and *Itga6*$^{-/-}$ spleens (Fig. 5*B*).

As Notch2 is crucial for MZ B-cell development and *Deltex1* expression is strictly dependent on that of Notch2 (13), we examined the expression of *Deltex1* mRNA in sorted MZ, FO, and NF B cells isolated from conditional *Lama5*$^{-/-}$ and *Itga6*$^{-/-}$ chimeric mice spleens, revealing an unexpected up-regulation of *Deltex1* in NF cells in both cases (Fig. 5*C*; Fig. S11*B*). Flow cytometry of sorted NF B cells revealed two populations, one consisting of small sized cells and a second population consisting of cells as large as mature MZ B cells, which expressed 10-fold more *Deltex1* than the small NF B cells, at levels comparable to mature MZ B cells (Fig. 5*D*; Fig. S11*C*). Staining for additional surface markers revealed that the large NF cells were

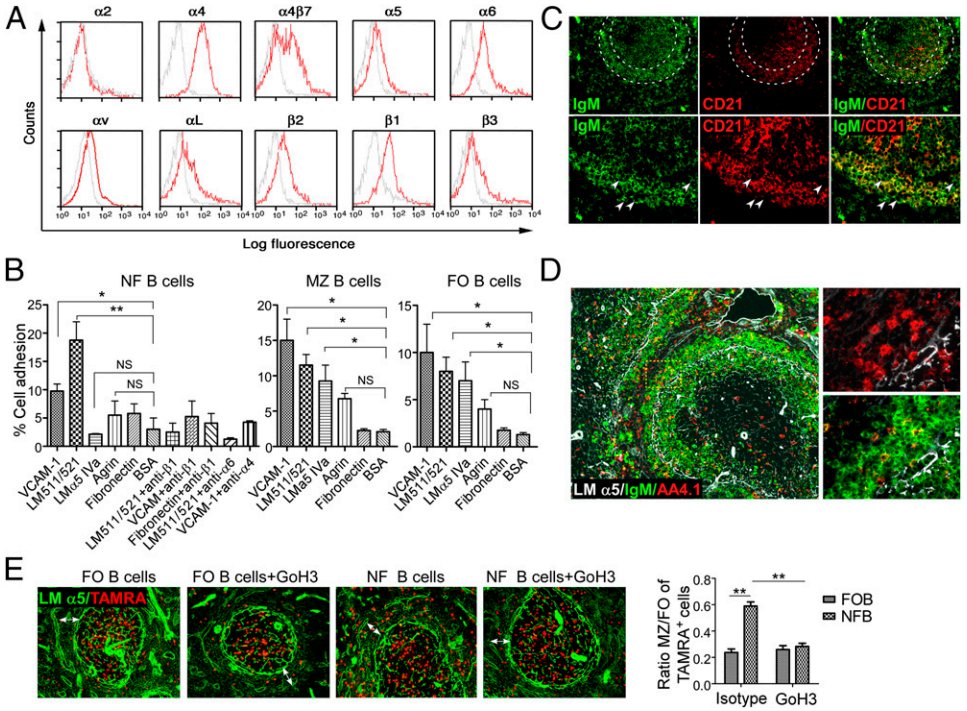

Fig. 3. NF B cells express laminin α5 binding integrins and show some colocalization with laminin α5 in the MZ. (*A*) Representative flow cytometry for cell surface integrin expression on NF B cells with antibody isotype controls shown in gray. (*B*) In vitro adhesion of MZ, FO, and NF B cells to VCAM-1, laminin 511/521, the RGD-containing laminin α5 domain IVa, agrin, fibronectin (all 30 μM), or BSA. Adhesion of NF B cells to VCAM-1, laminin 511/521, or fibronectin was measured in the presence or absence of function blocking antibodies to integrins β1 (Ha2/5), α6 (GoH3), or α4 (PS/2). Data shown are mean values ± SEM from three separate experiments with $n = 6$ for each treatment in each experiment. (*C*) Immunofluorescence staining shows the presence of IgM$^+$CD21^{low} and (*D*) IgM$^+$AA4.1$^+$ B cells in the MZ of mature mice (arrowheads). Magnification, 100× (*D*, *Left*), 200× (*C*, *Upper*), 400× (*C*, *Lower*, and *D*, *Right*). (*E*) In vivo localization of ex vivo TAMRA-labeled NF B cells or FO B cells (isolated from day 10 mouse spleens) at 16 h after i.v injection into mature mice in the presence or absence of GoH3. Immunofluorescent staining for laminin α5 reveals localization of NF B cells in the MZ (double arrows), follicle, and RP, whereas FO B cells home predominantly to the follicle. Coinjection with GoH3 reduced TAMRA$^+$ NF B-cell localization to the MZ only. Magnification: 100×. Bar graph shows quantification of the ratio of MZ/FO localized TAMRA$^+$ cells; data are means ± SEM from two experiments with four mice in each category. $*P < 0.05$; $**P < 0.01$.

IgM$^+$CD1d^{neg}HAS^{high} and some were also AA4.1$^+$ (Fig. 5*E*) and, therefore, probably represent an intermediate developmental phase between the conventional NF B cells (small) and MZ B cells. This result suggests that integrin α6β1-mediated binding to laminin α5 is not a prerequisite for Notch2-dependent differentiation of NF B cells to MZ B cells, but may act with other factors to support this differentiation. To test this hypothesis, CD21^{low}/CD23^{low} NF B cells isolated from 10-d-old mouse spleens were incubated in the presence of soluble laminin 511 or agrin, with and without added BAFF. Agrin also carries growth factor binding domains but cannot bind integrin α6β1 (31). Cells were incubated for 48 h at 37 °C with the ECM molecules in the presence or absence of GoH3 anti-integrin α6 or isotype control antibody, and numbers of NF vs. MZ B cells were measured by flow cytometry; control experiments involved incubation with BAFF alone or ECM molecules not expressed at this site (laminin 411). MZ B-cell differentiation was assessed by determining proportions of CD21^{high}/CD1d^{high} and CD23$^+$/CD21$^+$ cells; IgM/IgD cannot distinguish between NF and MZ B cells (both IgM^{high}IgD^{low}) but permitted investigation of FO B cells (IgM$^+$/IgD^{high}). To exclude the possibility that survival of contaminating MZ B cells in the NF B-cell preparation may contribute to the results, the same experiments were performed with sorted mature MZ B cells. Fig. S12 shows flow cytometry analyses of the MZ and NF B-cell populations before and after 48-h culture. In contrast to the NF B cells, where a small but consistent proportion of the cells survived the 48-h incubation period, none of the MZ B cells survived, regardless of the presence of BAFF or ECM molecules.

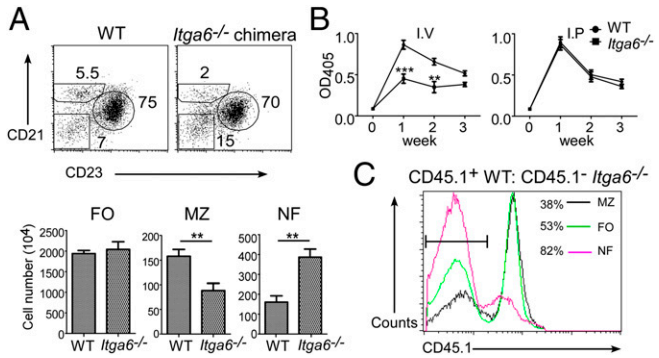

Fig. 4. WT mice carrying *Itga6*$^{-/-}$ bone marrow show reduced MZ B-cell and increased NF B-cell frequencies. (*A*) Representative flow cytometry of CD21^{low}CD23^{low} NF B cells, CD21^{high}CD23^{low} MZ B cells, and CD21^{high}CD23^{high} FO B cells in the spleen of the bone marrow chimeric mice at 10 wk after reconstitution, with corresponding quantification of absolute numbers of NF, MZ, and FO B cells (data are means of three experiments with five mice per experiments ± SEM; $**P < 0.01$. (*B*) Circulating IgM levels in *Itga6*$^{-/-}$ chimeric mice and WT controls (WT mice carrying WT bone marrow) in response to i.v. or i.p. immunization with T cell-independent antigen (NP-Ficoll). Data shown are means ± SEM from eight *Itga6*$^{-/-}$ chimeras and WT controls and three independent experiments. $**P < 0.01$; $***P < 0.001$. (*C*) Competitive bone marrow reconstitution studies were performed with a 1:1 ratio of CD45.1$^+$ WT: CD45.2$^+$ *Itga6*$^{-/-}$ bone marrow cells injected i.v. into WT irradiated mice and subsequent analysis of CD45.1$^+$ (WT) or CD45.1$^-$ (*Itga6*$^{-/-}$) cells in NF, MZ, and FO B-cell compartments, showing preferential accumulation of *Itga6*$^{-/-}$ cells in the NF B-cell compartment. Percentages of *Itga6*$^{-/-}$ B cells within the different B-cell subpopulations are shown.

Indeed, IgM$^+$ cells are those predestined to die (32), these data also indicate

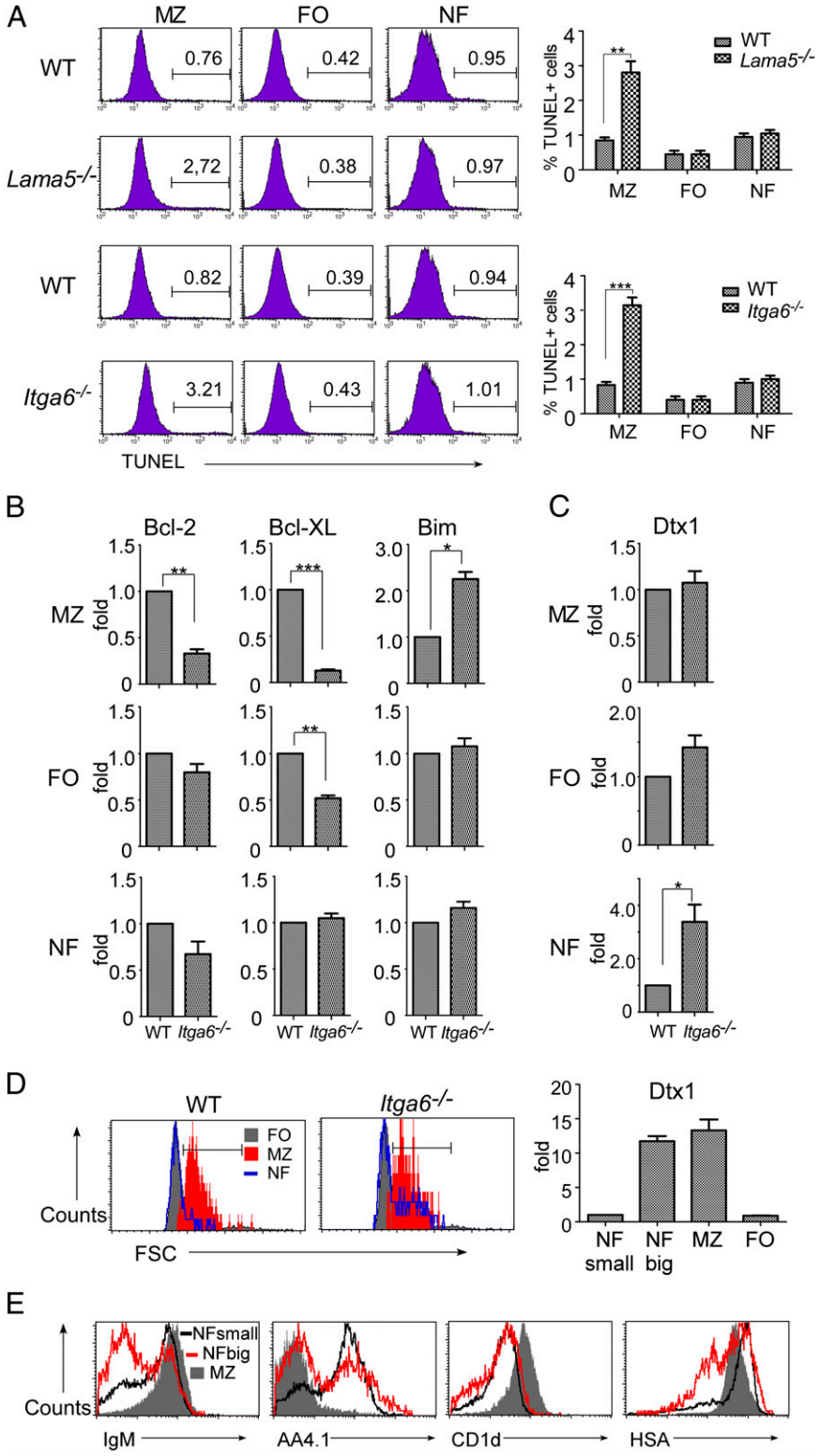

Fig. 5. Integrin α6β1-laminin α5 interactions support MZ B-cell determination and survival in vivo. (*A*) Representative flow cytometry of TUNEL-positive NF, MZ, and FO B cells in the spleens of conditional *Lama5*$^{-/-}$ and *Itga6*$^{-/-}$ bone marrow chimeric mice showing increased apoptosis of MZ B cells only. Bar graphs show means ± SEM from at least three separate experiments with three to four mice per experiment. (*B*) qRT-PCR for antiapoptotic (Bcl-XL, Bcl-2) and proapoptoic (Bim) genes in NF, MZ, and FO B cells in the spleens of *Itga6*$^{-/-}$ bone marrow chimeric mice. Data shown are fold differences from WT mice, $n = 3$ experiments, with triplicates in each. (*C*) qRT-PCR for Deltex-1 (Dtx1) in NF, MZ, and FO B cells sorted from the spleens of *Itga6*$^{-/-}$ bone marrow chimeric mice, showing up-regulation in NF B cells. Data shown are fold differences from WT mice; $n = 3$ experiments. (*D*) Forward scatter (FSC) of sorted NF, MZ, and FO B cells from the spleens of *Itga6*$^{-/-}$ bone marrow chimeric mice reveals a population of small Dtx1-negative NF B cells and larger cells of similar to mature MZ B cells that are Dtx1 positive. Bar graph shows fold differences compared with FO B cells, $n = 3$ experiments, with triplicates in each. $^{*}P < 0.05$; $^{**}P < 0.01$;$^{***}P < 0.001$. (*E*) Surface levels of IgM, AA4.1, CD1d, and HSA on the gated large (FSC^{high}), small (FSC^{low}), and MZ B-cell populations are also shown.

that both BAFF and laminin 511, but not agrin, promote immature B-cell survival (Fig. 6*B*).

To test whether interactions with laminin 511 support NF B-cell differentiation toward the MZ compartment in vivo, sorted CD45.2^{+}CD21^{low}/CD23^{low} NF B cells were transferred i.v. to mature (8–9 wk) CD45.1^{+} mice. NF B cells were precincubated with GoH3 or isotype control antibody before transfer, and the appearance of CD45.2^{+} cells in NF, MZ, and FO B-cell compartments was measured at 7 d by flow cytometry. Approximately 4% of the donor cells were recovered in the spleens. Fig. 6*C* shows that CD45.2^{+} donor cells accumulated in the MZ B-cell compartment, but when transferred cells were preincubated with GoH3, this was significantly reduced and was accompanied by an increase of CD45.2^{+} cells in the NF B-cell compartment, prob-

ably reflecting remaining transferred cells. These results suggest that integrin α6β1-mediated interaction between NF B cells and laminin α5 in vivo may promote differentiation to MZ B cells.

ELISA performed using laminin 511, agrin, laminin 411, or fibronectin as substrates revealed binding of BAFF only to the MZ-specific ECM molecules laminin 511 and agrin (Fig. 6*D*). Confocal microscopy of isolated NF B cells plated on laminin 511 or laminin 511 plus BAFF showed clustering of the integrin α6β1 receptor and colocalization of BAFF receptors within these clusters, whereas BAFF alone or agrin did not cluster the BAFF receptors or integrin α6β1 (Fig. 6*E*). Control experiments performed with the highly adhesive substrate, VCAM-1, showed no clustering of integrin α6β1 or BAFF receptors (Fig. 6*E*). To better define the BAFF receptor involved, transmembrane activator and CAML interactor (TACI), which also binds BAFF, is highly expressed on MZ B cells and clusters on engagement of its ligand a proliferation-inducing ligand (APRIL) (33), was also investigated. TACI$^{-/-}$ cells showed the same pattern of results as obtained with WT cells, which does not exclude the involvement of TACI but indicates that clustering of integrin α6β1 and BAFF receptors can also occur in its absence. The fact that agrin can bind BAFF to the same extent as laminin α5 (Fig. 6*D*) but cannot promote the mature MZ B cells (Fig. 6*A*) or cluster BAFF receptors, indicates that it is not simply ECM binding and enrichment of BAFF that supports the MZ B-cell population but rather highlights the importance of laminin α5–integrin α6β1-mediated signaling in the synergistic effects of BAFF and laminin α5.

Discussion

In addition to cell adhesion molecules and chemotactic gradients, we show that the MZ is characterized by a unique ECM occurring pericellularly around individual stromal cells to form a filligree halo extending from the marginal sinus, the main constituents of which are the basement membrane glycoproteins, laminin α5 (laminin 511/521), and the heparan sulfate, agrin. Although other ECM molecules occur at this site, including collagen type IV, nidogen 1, fibronectin, perlecan, and an as yet undefined molecule detected by the ERTR7 antibody, they are also expressed in the RP stroma, and only laminin α5 distribution correlates with MZ B-cell localization and size of this compartment.

Analyses of transgenic mice with expanded or absence of the MZ B-cell compartment showed that the localization of MZ B cells coincides precisely with the laminin α5–positive areas and that laminin α5 is lost when MZ B cells are absent. Interestingly, the absence of laminin α5 in the MZ of CD19$^{-/-}$ mice suggests that MZ B-cell presence may contribute to the maintence of laminin α5 expression in the MZ in a positive feedback fashion, potentially via cytokine induced mechanisms as has been shown

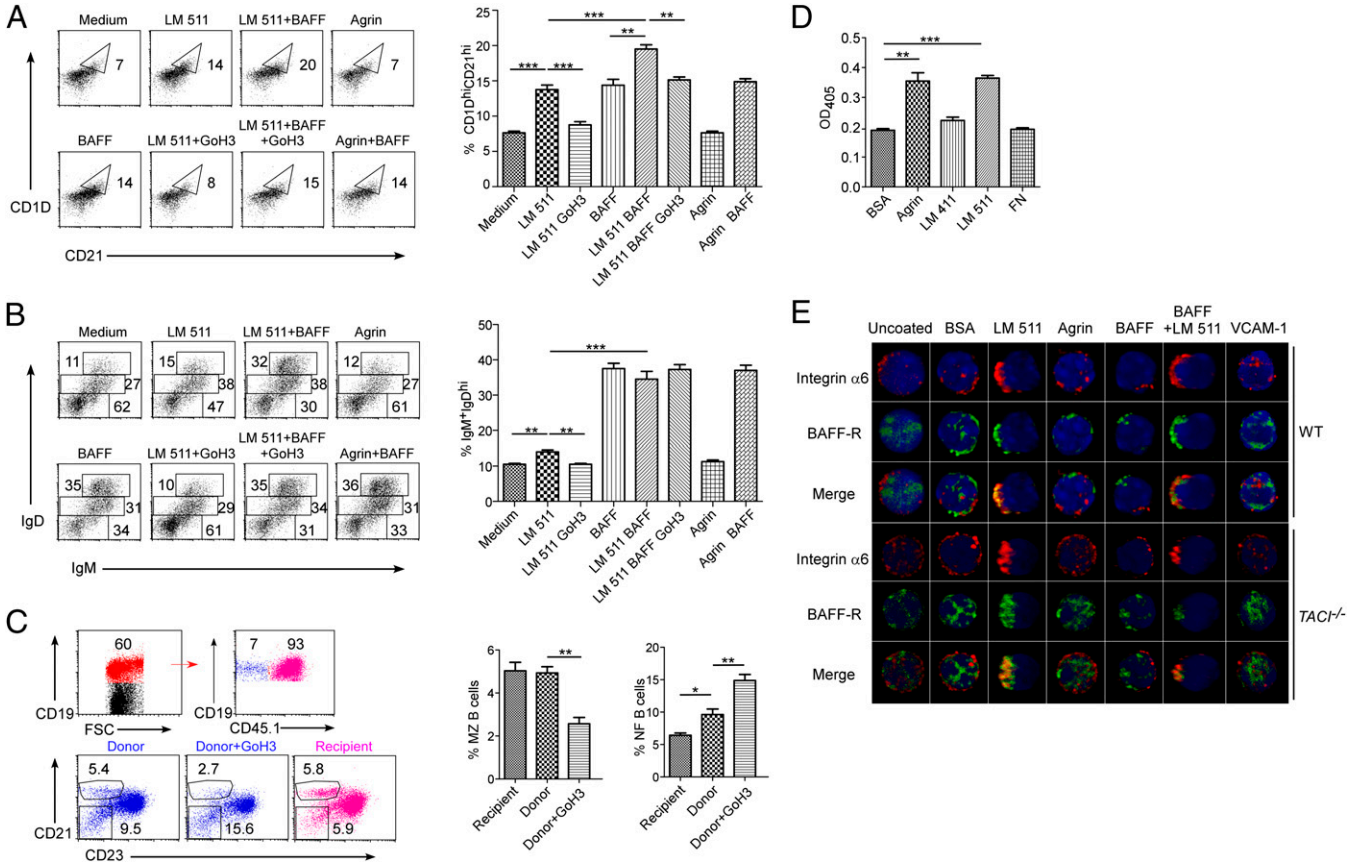

Fig. 6. Laminin α5 supports formation of MZ B cells in vitro and in vivo. Representative flow cytometry for (*A*) CD1d/CD21 and (*B*) IgM/IgD of sorted CD19$^+$CD21^{low}CD23^{low} NF B cells after 48-h culture in the presence of BAFF, laminin 511, agrin, or different combinations thereof, in the presence or absence of GoH3. Gatings in *A* and *B* were on live cells. Bar graphs show quantitative data from all experiments performed; $n = 3$ experiments, with triplicates in each; $^{**}P < 0.01$, $^{***}P < 0.001$. (*C*) Sorted CD45.2$^+$ NF B cells were transferred into adult CD45.1$^+$ recipients in the presence or absence of GoH3, and spleens were analyzed at day 7. Spleen cells were sorted by FSC and gated on CD19$^+$ cells and subsequently separated into CD45.1$^+$ and CD45.1$^-$ populations, which were analyzed for CD21/CD23 levels to define MZ and NF B cells. Bar graph shows proportions of MZ and NF B cells from four experiments with four mice per experiment; data shown are means ± SEM; $^*P < 0.05$, $^{**}P < 0.01$. (*D*) ELISA for the binding of BAFF to Agrin, laminins 411 and 511, and fibronectin (FN). Data shown are means of three experiments with triplicates in each experiment. $^{**}P < 0.01$, $^{***}P < 0.001$. (*E*) Confocal microscopy of NF B cells isolated from WT and TACI$^{-/-}$ mice were plated on plastic alone or culture dishes coated with BSA, agrin, VCAM-1, laminin 511, or BAFF alone or BAFF bound to laminin 511. Cells were double stained for integrin α6 and BAFF receptors. Magnification: 600×.

in other systems (34). Although MZ B cells bind to laminin α5 in in vitro assays via β1 and β3 integrins, the results of in vivo dislodgement studies indicate that this does not contribute to long-term retention of MZ B cells or other MZ resident cells to this site, as has been shown for VCAM-1 and ICAM-1 for MZ B cells (10). Rather, analysis of the *Lama5*$^{-/-}$ mouse lacking laminin α5 in the MZ suggests that interactions of the immigrating NF B cells with laminin α5 in the MZ promotes survival of MZ B cells and potentially also their formation. In vitro and in vivo studies suggest that NF B cells use integrin α6β1 to interact with laminin α5 in the unique ECM of the MZ and that at least transient passage of immigrating NF B cells through this compartment promotes the MZ B-cell lineage, as previously suggested (8).

Loss of either laminin α5 in the MZ or integrin α6 on B cells results in the same reduction in the mature MZ B-cell population and in an impaired antibody response to T-cell independent antigen, consistent with defective MZ B-cell function. Both the conditional *Lama5*$^{-/-}$ mouse and mice carrying *Itg6*$^{-/-}$ bone marrow showed no changes in FO B-cell numbers or in other MZ resident cells, including MZ macrophages or sinus-lining macrophages. Nor were there abnormalities in expression patterns of adhesion molecules known to play a role in MZ retention, including VCAM-1 and ICAM-1, consistent with the absence of defects on MZ B-cell retention. The increase in the proportion of T1 and reduction in T2 transitional B cells, coupled with the absence of a defect in pre- and pro-B cells or in immature B cells in the bone marrow, indicates that early B-cell development is not affected by reduced laminin α5 expression in the MZ or loss of integrin α6β1 on B cells but that the transition from T1 to T2 in the spleen is impaired, leading to a subsequent decrease in mature MZ B-cell numbers.

Existing data suggest that T1 cells give rise to T2 cells, which subsequently give rise to FO and MZ B cells, possibly via a third transitional population (T3), and that both positive and negative regulatory pathways within the spleen control the final outcome of these populations. The T1 population is considered to be negatively regulated within the spleen, with BCR signals leading to cell death, whereas T2 cells are positively regulated with BCR signaling, leading to their differentiation (35). In addition, mutations in the BAFF receptor and the canonical NF-κB signaling pathway, Notch2, or signaling molecules linked to integrin or chemokine activation all lead to reduced MZ B-cell numbers (36). Our data suggest that integrin α6β1–laminin α5 interactions are additional factors that impact on T1 and T2 fate and that it is the threshold of signals collectively arising from several sources that determines whether the final MZ phenotype results. Our data suggest that transient retention of NF B cells in the MZ via integrin α6β1–laminin α5-mediated interactions promotes T1 to T2 transition and hence MZ B-cell formation; however, given that the NF B cells also bind VCAM-1, this may also be provided by VCAM-1/α4β1 interactions in the absence of either laminin α5 or integrin α6β1, explaining why not all MZ B cells are lacking in the *Lama5*$^{-/-}$ and *Itg6*$^{-/-}$ chimeric mice. Similarly, the existence of small and large NF B cells in mice lacking laminin α5 in the MZ or integrin α6β1, the larger of which expressed several NF B-cell markers and downstream genes of Notch2 signaling (*Deltex-1*) and were therefore committed to the MZ B-cell lineage, suggests that integrin α6β1-mediated binding to laminin α5 is not a prerequisite for Notch2-dependent differentiation of NF B cells to MZ B cells, but may be one of several factors that promote this step.

TUNEL experiments clearly show that integrin α6β1-mediated interaction of mature MZ B cells with laminin α5 promotes their survival. Our in vitro experiments revealed that laminin 511 was almost as effective as BAFF and synergizes with BAFF in supporting the survival of NF B cells, as well as promoting NF B-cell differentiation toward the MZ compartment. These results suggest that integrin α6β1-mediated laminin α5 interactions may directly promote MZ B-cell differentiation in vivo. However, taken together with the reduced survival of MZ B cells in *Lama5*$^{-/-}$ and *Itg6*$^{-/-}$ chimeric mice, the reduced numbers of MZ B cells in these mice could also be explained by an altered turnover of MZ B cells. These different possibilities cannot be resolved without in vivo BrdU-labeling experiments. The fact that agrin can bind BAFF to the same extent as laminin 511 but does not support the MZ B-cell population in in vitro experiments, nor cluster BAFF receptors, indicates that laminin α5 does not act by simply binding and enriching BAFF, but rather suggests synergistic effects of laminin α5 and BAFF. As BAFF promotes B-cell survival, the synergistic effect of laminin 511 plus BAFF is likely to explain the elevated apoptosis of MZ B cells in mice lacking laminin α5 in the MZ or integrin α6β1 on B cells.

That laminin α5 directly binds BAFF and clusters BAFF receptors and integin α6β1, as shown here, suggests the formation of supramolecular membrane complexes where the integration of the MZ B-cell promoting signals from integrin α6β1 and BAFF receptors are amplified (Fig. 7). Data from our laboratory suggest that in the case of both BAFF and laminin α5, this involves induction of MAPK/ Erk1 signaling. Other examples exist where cell–matrix interactions amplify the effects of growth factors (37); for example, integrin α6β1-mediated contact of oligodendrocytes with axonal laminins results in the clustering of α6β1 and PDGF receptors into lipid rafts and amplifes PDGF-mediated induced oligodendrocyte maturation (38). However, this is first demonstration of such an effect on immune cell fate.

In addition to these direct effects of laminin α5, indirect effects are likely. In this context, it is noteworthy that laminin α5 forms a filigree connection between the MZ and the basement membrane of the bordering venous sinuses (Fig. 1*B*) (4) and that exogenously injected TAMRA-labeled NF B cells localize not only to the MZ but also to the venous sinuses. Because Notch2 is required for MZ B-cell development but its ligand, Delta1, is mainly expressed on the endothelium of the venous sinuses in the RP (39), laminin α5 may also provide a pathway for shuttle between these sites. Preliminary data from our laboratory show that Delta1 is still expressed on the venous sinus endothelium of mice lacking laminin α5 at this site; hence, it is not required for Delta1 expression.

In addition to the effects on the immigrating NF B cells and MZ B cells, we demonstrate that FO B cells can also bind to laminin 511. The precise function of this interaction remains unclear, but may include transient retention of FO B cells in the MZ during their recirculation, which was previously suggested to be mediated by interaction with fibronectin (27) but, which we show here, is not an adhesive substrate for these cells.

Our data demonstrate that interactions with ECM do not necessarily translate to strong adhesion but rather can result in transduction of signals that affect processes such as differentiation

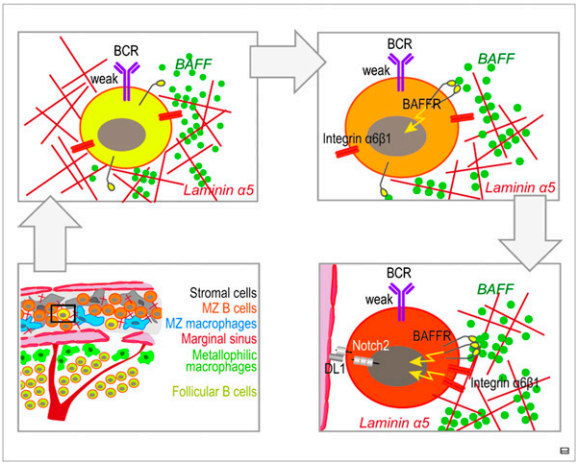

Fig. 7. Proposed model of how laminin α5-integrin α6β1-mediated interactions impact on the MZ B-cell population. NF transitional B cells immigrating from the bone marrow (yellow cells), characterized by weak B-cell receptor (BCR) signaling, arrive in the unique laminin α5-rich perifollicular network where they interact with laminin α5 via integrin α6β1. Laminin α5 can directly bind BAFF and clusters BAFF receptors (BAFFRs) and integin α6β1, resulting in supramolecular membrane complexes where the integration of NF and MZ B cell–promoting signals from integrin α6β1 and BAFF receptors are amplified, which together with the Notch2-dependent pathways support commitment to the MZ B-cell fate (large orange cells).

and survival. Although laminins have long been known to play such roles in differentiation of several tissue types, with their α chains being responsible for cell adhesion and biological activity (40), a role in immune cell development or homeostasis has not been previously demonstrated. Indeed, the function of the ECM of lymphoid organs has remained poorly studied, despite its abundance in these organs and enormous potential to interact with both cells and soluble cytokines, which has been due to the lack of tools and animal models to study the ECM of lymphoid organs and hence lack of information on its biochemical nature. We show here that the fine, perifollicular laminin α5 expression pattern in the spleen clearly defines a unique niche that supports the formation and survival of the highly specialized MZ B-cell population. Integrin α6β1-mediated interaction of NF B cells with laminin α5 in the MZ supports the MZ B-cell population and synergies with BAFF to enhance their long-term survival and physiological function (Fig. 7). Structurally similar ECM structures surround the stromal cells of the bone marrow, thymus, and fetal liver; the cell–matrix relationships described here are therefore likely to have broader ramifications to other immune cell fates.

Materials and Methods

Animals and Tissues. The following mice were on a C57BL/6 background and were used at 8–15 wk of age: WT C57BL/6, NOD mice (41), transgenic 24αβNOD mice expressing the Vα3.2Vβ9 TCR (42), $CD19^{-/-}$ mice (19), $agrin^{-/-}$ mice (43), and $TACI^{-/-}$ mice (44). A laminin α5 endothelial cell–specific KO mouse, generated by crossing a laminin α5 mouse carrying *lox P* flanking exons 2–4 (21) with the Tie-2 cre recombinase mouse (22), was used and is referred to as conditional $Lama5^{-/-}$ (Fig. S3). Animal breeding and experiments were conducted according to the Swedish and German Animal Welfare guidelines.

Immunofluorescence. Antibodies used in immunofluorescence studies recognizing ECM molecules are detailed in Table 1. Antibodies to the following were used to identify cellular compartments: B220 (Pharmingen), IgM and IgD (Pharmingen), ERTR9 and ERTR7 (BMA Biomedicals), MOMA-1 (BMA Biomedicals), MadCAM [mouse endothelial cell antigen (MECA)-367], ICAM-1 (YN1/1.7), VCAM-1 (M/K-2; Southern Biotech, and MVCAM.A; BD Biosciences), and CD21 (BD Biosciences). Secondary antibodies included donkey anti-goat FITC-conjugated IgG (Dianova), goat anti-hamster IgG Alexa Fluor 594 (Molecular Probes), goat anti-rabbit FITC-conjugated IgG, rhodamine-conjugated IgG (H+L) (Dianova), Cy5-conjugated IgG (Dianova), goat anti-rat Texas red–conjugated IgG, Alexa Fluor 594 IgG (Molecular Probes), donkey anti-rat Alexa Fluor 488 IgG, Cy3-conjugated IgG (H+L), and mouse anti-rat FITC-conjugated κ chain IgM (Immunotech). In some cases, mice were injected with 100 μg each of anti-integrin α4 (PS/2; Pharmingen) and anti–LFA-1 (M17/4; Pharmingen) to displace MZ B cells; after 3 h, spleens were collected, frozen, and stained for VCAM-1, ICAM-1, or laminin α5.

Spleens were frozen in Tissue Tek (Miles Laboratories) in isopentane at −70 °C. Five-micrometer cryostat sections were fixed for 10 min in −20 °C methanol. For confocal microscopy or 3D reconstructions, tissues were fixed in 1.5% (wt/vol) paraformaldehyde for 1.5 h at 4 °C and embedded in 1% (wt/vol) agarose, and 60- to 100-μm sections were prepared using a vibratome. Thick sections were treated with PBS plus 1% (wt/vol) BSA before overnight incubation with primary antibody at 4 °C. Immunofluorescence staining was carried out as described previously (34). Sections were examined using a Zeiss AxioImager microscope equipped with epifluorescent optics and documented using Hamamatsu ORCA ER camera or with a Zeiss confocal laser scanning system LSM 700. Images were analyzed using Volocity 6.0.1 software (Improvision).

Flow Cytometry. Single cell suspensions of splenocytes or bone marrow cells were obtained by sieving through a 70-μm filter. Splenocytes or bone marrow (10^6) cells were stained for integrins by first blocking Fc-receptors with 10% (vol/vol) normal goat and mouse serum (Sigma-Aldrich). The following unconjugated anti-integrin antibodies were used, purchased from BD Biosciences unless otherwise stated: α2 (HMα2, Dx5), α4β7 (DATK32), α4 (PS/2), α5 (X-6, Dianova), α6 (GoH3), αL (M17/4.2 ATCC), β1 (Ha2/5 and 9EG7), β2 (GAME-46), β3 (2C9.G2), lutheran blood group glycoprotein (45), and sulphatide (3′-sulphogalactosylceramide) (Sulph 1) (46), and isotype anti-rat and anti-hamster controls. Biotinylated polyclonal goat anti-rat Ig multiple adsorbed (Pharmingen) or biotinylated goat anti–Armenian hamster IgG (Jackson Immunoresearch Laboratories) was then added. Unspecific binding was further blocked by 10% (vol/vol) normal rat serum (Sigma-Aldrich), and in the final step, anti–CD21-FITC (Pharmingen), anti–CD23-phycoerythrin (PE) (Pharmingen), streptavidin-PerCP (Pharmingen), and anti–B220-Cy5 (RA3.6.B2, Pharmingen) were added.

Allophycocyanin (APC)-labeled anti-CD93 (AA4.1) (eBioscience), biotin- or PE-labeled anti-CD23, FITC- or PE-labeled anti-CD21, biotin-labeled anti-CD1d (Pharmingen), FITC-labeled anti-IgM, and PerCP-labeled anti-B220 (Pharmingen) were used for flow cytometry of transitional B-cell populations in the bone marrow and spleen. An in situ cell death detection kit (Roche) that detects TUNEL-positive cells was used to determine the proportion of apoptotic MZ and FO B cells in the spleens. Flow cytometry was performed on a FACSCalibur (Becton Dickinson), and data analysis was done using CellQuest software (BD Biosciences).

In Vitro Adhesion Assays. In vitro adhesion assays for MZ and FO B cells were performed as previously described (10) using the following substrates: purified laminin 511/521 (47) and recombinant agrin (43), as representatives of ECM molecules enriched in the marginal zone; fibronectin, which is present in the marginal zone and the RP; and VCAM-1 (ADP5; R&D Systems), which has previously been identified as an adhesive substrate for splenocytes (10). Recombinant laminin α5 fragments were used to define binding domains (domains IVa, G4–G5, V–VI) (23). All proteins were used at the same molar concentration (30 μM) and were plated at 37 °C for 1 h; wells were washed with PBS and blocked with 1% (wt/vol) BSA (A-3311; Sigma Aldrich) in PBS. Adhesion assays were performed at 37 °C for 90 min, and bound MZ and FO B cells were analyzed by flow cytometry using B220/CD1d/CD21/CD23 to distinguish cell populations (10). To examine the adhesion of NF B cells to ECM and VCAM-1, enriched splenic B lymphocytes obtained using anti-CD19–coated magnetic (MAC) beads (Miltenyi Biotech) were used in adhesion assays and adherent cells determined by FACS for $B220^+AA4.1^+$ cells.

To determine receptors mediating adhesion to the different substrates, cell adhesion assays were performed in the presence or absence of 25 μg/mL of blocking antibodies to integrins α6 (GoH3), β1 (Ha2/5), β3 (2C9.G2), α4 (PS/2), or cylic-RGD peptides, specific for αv series integrins, and control peptides (47).

In Vivo Homing and In Vivo Differentiation Assays. NF B cells ($CD19^+CD21^{low}CD23^{low}$) and FO B cells ($CD19^+CD23^{high}/CD21^{low}$) were isolated from spleens of day 10 mice. In some cases, cells were labeled with 5 μM 5(6)-TAMRA-SE (Invitrogen) before transfer to permit in vivo localization or were isolated from Ly5.1 mice and transferred to Ly5.2 recipients to permit in vivo quantification. Cells (5×10^6) were transferred per 8- to 9-wk-old recipient. Quantification of $TAMRA^+$ cells at 16 h after transfer in the spleens required sectioning of entire spleens and counting of $TAMRA^+$ cells in the different spleen compartments using either IgM^{high} or anti-laminin α5 as a marker of the MZ. At least 10 different areas per section and at least 20 sections per animal were counted.

For in vivo differentiation studies, 50×10^6 $CD45.2^+$ NF B cells were transferred per 8- to 9-wk-old CD45.1 recipient, and $\sim 2 \times 10^6$ cells were recovered in the spleen after 7 d. $CD45.2^+$ NF cells were preincubated with 50 μg/mL GoH3 or isotype control antibody for 1 h at 4 °C before injection. Spleen cells were analyzed by FSC and gated on $CD19^+$ cells and were subsequently separated into $CD45.1^+$ and $CD45.1^-$ populations, which were analyzed for CD21/CD23 levels to define MZ and NF B cells.

qRT-PCR. qRT-PCR was carried out on sorted MZ ($CD21^{high}CD23^{low}$), FO ($CD21^{high}$ $CD23^{high}$), and NF ($CD21^{low}CD23^{low}$) B cells for expression of Bcl-xl, Bcl-2, Bim, and Deltex1 (13).

Bone Marrow Chimeric Mice/Competitive Bone Marrow Reconstitution. As integrin α6 KO ($Itga6^{-/-}$) (30) mice die perinatally, bone marrow reconstitution was performed using embryonic day 16 liver cells from $Itga6^{-/-}$ embryos. $Itga6^{-/-}$ fetal liver cells ($10–15 \times 10^6$) (Ly5.2) were injected i.v. into lethally irradiated (11Gy) congenic WT recipient mice (Ly5.1). Engraftment took 8–10 wk, and mice with >95% donor cell engraftment were used. Competitive bone marrow reconstitution studies were performed with a 1:1 ratio of $CD45.1^+$ WT: $CD45.2^+$ $Itga6^{-/-}$ bone marrow injected i.v. into WT irradiated mice. Mice were analyzed at 10 wk after engraftment.

ELISA. Ninety-six-well ELISA plates were coated overnight at 4 °C with BSA, agrin, laminin 411, laminin 511, or fibronectin (3 μg/mL) and blocked with 2% (wt/vol) BSA, and BAFF (R&D 500 ng/mL) was added at room temperature for 2 h. Rat anti-BAFF (Abcam, 1 μg/mL) and HRP-conjugated goat anti-rat were used to detect bound BAFF.

Immunization/Antibody Response. Mice were immunized by i.v. or i.p. injections of 50 μg NP-Ficoll in a volume of 200 μL. At 1, 2, and 3 wk after immunization, serum antibody titers were measured using the Clonotyping System Kit (Southern Biotech).

In Vitro MZ B-Cell Differentiation. NF B cells (1×10^6; $CD19^+CD21^{low}CD23^{low}$) from spleens of day 10 mice were incubated with the following substrates for 48 h at 37 °C: 10 μg/mL of BSA, laminin 511, laminin 411 or agrin, 100 ng/mL BAFF, or combinations thereof. Control experiments involved isolation of $CD19^+CD21^{hi}CD23^{low}$ MZ B cells from adult spleens using FACSAria (BD Biosciences) and their culture under the same conditions as the NF B cells. Experiments were performed in the presence or absence of 50 μg/mL integrin α6 blocking antibody (GoH3). Cells were analyzed by flow cytometry using CD1d, CD21, CD23, IgM, and IgD antibodies. 7AAD (BD Biosciences) was used to identify dead cells.

Colocalization Assay. Coverslips were coated overnight at 4 °C with BSA, BAFF, agrin, VCAM, or laminin 511 alone (3 μM), or laminin 511 to which BAFF was subsequently bound by incubation at room temperature for 2 h. NF B cells (1×10^6) from WT or $TACI^{-/-}$ mice were added and incubated at 37 °C for 2 h. After washing, coverslips were fixed in 4% PFA, blocked with 2% BSA, and stained with anti-integrin α6, GoH3 (1 μg/mL), and anti-BAFF receptor (anti-CD268, clone ebio7H22-E16; eBioscience, 1 μg/mL). Bound antibodies were detected with Alexa488- or Cy3-conjugated secondary antibodies, and cells were examined using a Zeiss LSM 700 confocal laser scanning microscope. Images were analyzed using Volocity 6.0.1 software (Improvision).

Statistical Analyses. The data were analyzed by a paired sign *t* test or Student *t* test. All *P* values of 0.05 or less were considered statistically significant.

ACKNOWLEDGMENTS. We thank A. Ljubimov, R. Nischt, J.-E. Månsson, and D. Vestweber for generous gifts of antibodies; Pascal Schneider, Fabienne Mackay, and Biogen Idec Inc. for the $TACI^{-/-}$ mice; S. Budny for preparing laminins 511/521, 411, and laminin fragments; Adèle De Arcangelis for preparation of the integrin $\alpha6^{-/-}$ fetal livers; and Nina Gerigk for Fig. 7. This work was supported by the German [Sonderforschungsbereich (SFB) 492 A19] and Swedish Research Foundations (K2005-06X-14184-04A, 621-2001-2142), Alfred Österlunds, Knut and Alice Wallenbergs (KAW 2002.0056) and National Insitutes of Health Grant AI01478-33.

1. Ruhrberg C, et al. (2002) Spatially restricted patterning cues provided by heparin-binding VEGF-A control blood vessel branching morphogenesis. *Genes Dev* 16(20):2684–2698.
2. Sixt M, et al. (2005) The conduit system transports soluble antigens from the afferent lymph to resident dendritic cells in the T cell area of the lymph node. *Immunity* 22(1): 19–29.
3. Gretz JE, Norbury CC, Anderson AO, Proudfoot AE, Shaw S (2000) Lymph-borne chemokines and other low molecular weight molecules reach high endothelial venules via specialized conduits while a functional barrier limits access to the lymphocyte microenvironments in lymph node cortex. *J Exp Med* 192(10):1425–1440.
4. Lokmic Z, et al. (2008) The extracellular matrix of the spleen as a potential organizer of immune cell compartments. *Semin Immunol* 20(1):4–13.
5. Bajénoff M, Glaichenhaus N, Germain RN (2008) Fibroblastic reticular cells guide T lymphocyte entry into and migration within the splenic T cell zone. *J Immunol* 181(6): 3947–3954.
6. Nolte MA, et al. (2003) A conduit system distributes chemokines and small blood-borne molecules through the splenic white pulp. *J Exp Med* 198(3):505–512.
7. Martin F, Kearney JF (2002) Marginal-zone B cells. *Nat Rev Immunol* 2(5):323–335.
8. Cinamon G, Zachariah MA, Lam OM, Foss FW, Jr., Cyster JG (2008) Follicular shuttling of marginal zone B cells facilitates antigen transport. *Nat Immunol* 9(1):54–62.
9. Cancro MP, Kearney JF (2004) B cell positive selection: Road map to the primary repertoire? *J Immunol* 173(1):15–19.
10. Lu TT, Cyster JG (2002) Integrin-mediated long-term B cell retention in the splenic marginal zone. *Science* 297(5580):409–412.
11. Cinamon G, et al. (2004) Sphingosine 1-phosphate receptor 1 promotes B cell localization in the splenic marginal zone. *Nat Immunol* 5(7):713–720.
12. Allman D, Pillai S (2008) Peripheral B cell subsets. *Curr Opin Immunol* 20(2):149–157.
13. Saito T, et al. (2003) Notch2 is preferentially expressed in mature B cells and indispensable for marginal zone B lineage development. *Immunity* 18(5):675–685.
14. Engel P, et al. (1995) Abnormal B lymphocyte development, activation, and differentiation in mice that lack or overexpress the CD19 signal transduction molecule. *Immunity* 3(1):39–50.
15. Otero DC, Anzelon AN, Rickert RC (2003) CD19 function in early and late B cell development: I. Maintenance of follicular and marginal zone B cells requires CD19-dependent survival signals. *J Immunol* 170(1):73–83.
16. Guinamard R, Okigaki M, Schlessinger J, Ravetch JV (2000) Absence of marginal zone B cells in Pyk-2-deficient mice defines their role in the humoral response. *Nat Immunol* 1(1):31–36.
17. Mueller SN, Germain RN (2009) Stromal cell contributions to the homeostasis and functionality of the immune system. *Nat Rev Immunol* 9(9):618–629.
18. Rolf J, et al. (2005) The enlarged population of marginal zone/CD1d(high) B lymphocytes in nonobese diabetic mice maps to diabetes susceptibility region Idd11. *J Immunol* 174(8):4821–4827.
19. Rickert RC, Rajewsky K, Roes J (1995) Impairment of T-cell-dependent B-cell responses and B-1 cell development in CD19-deficient mice. *Nature* 376(6538):352–355.
20. Gautam M, et al. (1996) Defective neuromuscular synaptogenesis in agrin-deficient mutant mice. *Cell* 85(4):525–535.
21. Miner JH, Cunningham J, Sanes JR (1998) Roles for laminin in embryogenesis: Exencephaly, syndactyly, and placentopathy in mice lacking the laminin alpha5 chain. *J Cell Biol* 143(6):1713–1723.
22. Kisanuki YY, et al. (2001) Tie2-Cre transgenic mice: A new model for endothelial cell-lineage analysis in vivo. *Dev Biol* 230(2):230–242.
23. Sasaki T, Timpl R (2001) Domain IVa of laminin alpha5 chain is cell-adhesive and binds beta1 and alphaVbeta3 integrins through Arg-Gly-Asp. *FEBS Lett* 509(2):181–185.
24. Kikkawa Y, Sanzen N, Fujiwara H, Sonnenberg A, Sekiguchi K (2000) Integrin binding specificity of laminin-10/11: Laminin-10/11 are recognized by alpha 3 beta 1, alpha 6 beta 1 and alpha 6 beta 4 integrins. *J Cell Sci* 113(Pt 5):869–876.
25. Durbeej M (2010) Laminins. *Cell Tissue Res* 339(1):259–268.
26. Li S, et al. (2005) Laminin-sulfatide binding initiates basement membrane assembly and enables receptor signaling in Schwann cells and fibroblasts. *J Cell Biol* 169(1):179–189.
27. Lo CG, Lu TT, Cyster JG (2003) Integrin-dependence of lymphocyte entry into the splenic white pulp. *J Exp Med* 197(3):353–361.
28. Henderson RB, et al. (2010) A novel Rac-dependent checkpoint in B cell development controls entry into the splenic white pulp and cell survival. *J Exp Med* 207(4):837–853.
29. Loder F, et al. (1999) B cell development in the spleen takes place in discrete steps and is determined by the quality of B cell receptor-derived signals. *J Exp Med* 190(1):75–89.
30. Georges-Labouesse E, et al. (1996) Absence of integrin alpha 6 leads to epidermolysis bullosa and neonatal death in mice. *Nat Genet* 13(3):370–373.
31. Iozzo RV, Zoeller JJ, Nyström A (2009) Basement membrane proteoglycans: Modulators Par Excellence of cancer growth and angiogenesis. *Mol Cells* 27(5):503–513.
32. Kraus M, Alimzhanov MB, Rajewsky N, Rajewsky K (2004) Survival of resting mature B lymphocytes depends on BCR signaling via the Igalpha/beta heterodimer. *Cell* 117(6): 787–800.
33. He B, et al. (2010) The transmembrane activator TACI triggers immunoglobulin class switching by activating B cells through the adaptor MyD88. *Nat Immunol* 11(9):836–845.
34. Sixt M, et al. (2001) Endothelial cell laminin isoforms, laminins 8 and 10, play decisive roles in T cell recruitment across the blood-brain barrier in experimental autoimmune encephalomyelitis. *J Cell Biol* 153(5):933–946.
35. Allman D, et al. (2001) Resolution of three nonproliferative immature splenic B cell subsets reveals multiple selection points during peripheral B cell maturation. *J Immunol* 167(12):6834–6840.
36. Pillai S, Cariappa A (2009) The follicular versus marginal zone B lymphocyte cell fate decision. *Nat Rev Immunol* 9(11):767–777.
37. Comoglio PM, Boccaccio C, Trusolino L (2003) Interactions between growth factor receptors and adhesion molecules: Breaking the rules. *Curr Opin Cell Biol* 15(5):565–571.
38. Colognato H, et al. (2002) CNS integrins switch growth factor signalling to promote target-dependent survival. *Nat Cell Biol* 4(11):833–841.
39. Tan JB, et al. (2009) Lunatic and manic fringe cooperatively enhance marginal zone B cell precursor competition for delta-like 1 in splenic endothelial niches. *Immunity* 30(2):254–263.
40. Miner JH, Yurchenco PD (2004) Laminin functions in tissue morphogenesis. *Annu Rev Cell Dev Biol* 20:255–284.
41. Leiter EH, Prochazka M, Coleman DL (1987) The non-obese diabetic (NOD) mouse. *Am J Pathol* 128(2):380–383.
42. Duarte N, et al. (2004) Prevention of diabetes in nonobese diabetic mice mediated by CD1d-restricted nonclassical NKT cells. *J Immunol* 173(5):3112–3118.
43. Eusebio A, Oliveri F, Barzaghi P, Ruegg MA (2003) Expression of mouse agrin in normal, denervated and dystrophic muscle. *Neuromuscul Disord* 13(5):408–415.
44. Ng LG, et al. (2004) B cell-activating factor belonging to the TNF family (BAFF)-R is the principal BAFF receptor facilitating BAFF costimulation of circulating T and B cells. *J Immunol* 173(2):807–817.
45. Kikkawa Y, Moulson CL, Virtanen I, Miner JH (2002) Identification of the binding site for the Lutheran blood group glycoprotein on laminin alpha 5 through expression of chimeric laminin chains in vivo. *J Biol Chem* 277(47):44864–44869.
46. Fredman P, et al. (1988) Characterization of the binding epitope of a monoclonal antibody to sulphatide. *Biochem J* 251(1):17–22.
47. Sixt M, Hallmann R, Wendler O, Scharffetter-Kochanek K, Sorokin LM (2001) Cell adhesion and migration properties of β 2-integrin negative polymorphonuclear granulocytes on defined extracellular matrix molecules. Relevance for leukocyte extravasation. *J Biol Chem* 276(22):18878–18887.
48. Kohfeldt E, Sasaki T, Göhring W, Timpl R (1998) Nidogen-2: A new basement membrane protein with diverse binding properties. *J Mol Biol* 282(1):99–109.
49. Aufderheide E, Ekblom P (1988) Tenascin during gut development: Appearance in the mesenchyme, shift in molecular forms, and dependence on epithelial-mesenchymal interactions. *J Cell Biol* 107(6 Pt 1):2341–2349.